Iranian Journal of Materials Forming 11 (1) (2024) 24-33

Online ISSN: 2383-0042

IJMF

Iranian Journal of Materials Forming

Journal Homepage: http://ijmf.shirazu.ac.ir

Research Article

The Effect of Simple Shear Extrusion on the Microstructure and Surface Properties of Aluminum Components Produced by Powder Metallurgy

S.M. Sedehi[1], M. Samarghandi[2], A. Samarghandi[3] and M. Maraki[4*]

[1] School of Mechanical Engineering, College of Engineering, University of Tehran, Tehran, Iran
[2] Department of Mechanical Engineering, Birjand University, Birjand, Iran
[3] Department of Railway Engineering, Iran University of Science and Technology, Tehran, Iran
[4] Department of Materials Engineering, Birjand University of Technology, Birjand, Iran

ARTICLE INFO

Article history:

Received 14 February 2024
Reviewed 6 April 2024
Revised 4 May 2024
Accepted 11 May 2024

Keywords:

Aluminum
Severe plastic deformation
Powder metallurgy
Simple shear extrusion
Wear

Please cite this article as:

Sedehi, S.M., Samarghandi, M., Samarghandi, A., & Maraki, M. (2024). The effect of simple shear extrusion on the microstructure and surface properties of aluminum components produced by powder metallurgy. *Iranian Journal of Materials Forming*, *11*(1) 24-33. https://doi.org/10.22099/IJMF.2024.49501.1282

ABSTRACT

This study focuses specifically on the combination of two methods: powder metallurgy and severe plastic deformation. In this research, the influence of a single pass of simple shear extrusion (SSE) on the grain refinement, structural evolution, and some tribological properties of pure aluminum samples produced through the powder metallurgy method has been investigated. It is observed that after a single pass through the channel of SSE, the average grain size decreases, and the tribological properties of the sample significantly increases. The innovation of this research lies in the simultaneous combination of two methods: Fabrication of samples through powder metallurgy and severe plastic deformation. These methods lead to the alignment or even enhancement of the properties of the produced samples compared to conventionally cast samples. The recorded hardness values for the produced samples decreased from 57 Brinell for the as-cast sample to 29, 43, and 60.3 Brinell after initial pressing, sintering, and a single pass of SSE, respectively. Wear test results also indicate a substantial improvement in wear resistance in the refined-grain sample, with a weight loss reduction of 0.011 grams compared to the powder metallurgy stage. Furthermore, corrosion test results show an increase in corrosion potential from 730 to 720 millivolts in the powder metallurgy sample after SSE, and the current density decreases from 1.71 to 1.54 amperes per square centimeter in the powder metallurgy and simple shear extrusion samples, respectively.

1. Introduction

Due to their lightweight and excellent corrosion resistance, aluminum and its alloys are widely used in aerospace, automotive, and rail transportation industries [1]. The performance of aluminum alloys is closely related to their microstructural characteristics. Therefore, mastering the evolution law related to the microstructure of aluminum alloys during deformation is crucial for the precise production of products that meet performance requirements [2]. Generally, casting methods are used to synthesize aluminum and its alloys. However, casting methods often result in segregation and finer cracks. Hence, aluminum alloys are frequently produced through powder metallurgy methods, which are not only suitable for producing bulk alloy materials without segregation but also for homogeneous microstructures in complex components

* Corresponding author
E-mail address: maraki@birjandut.ac.ir (M. Maraki)
https://doi.org/10.22099/IJMF.2024.49501.1282

[3]. Powder metallurgy processes offer advantages such as low process temperature, low energy consumption, and high material utilization compared to other methods used for composite fabrication [4]. In powder metallurgy processes, reinforcing materials are mixed with matrix materials and compressed with sufficient pressure (depending on the required porosity in the final materials) to create cohesive components [5]. Then, the compressed samples are heated at a temperature usually below the melting point of the matrix material for a sufficient duration to allow particle bonding [6]. The heating and holding process at a predetermined temperature for a specific period is known as 'sintering' [7]. The amount of pressure, temperature, and sintering time are among the most critical parameters in the powder metallurgy process [8]. On the other hand, the unique physical and mechanical properties of ultrafine-grained materials make them an attractive subject for many contemporary scientific studies. Among various methods for processing such materials, severe plastic deformation methods are more favored as they provide bulk nanostructured materials without contamination or porosity [9, 10]. Methods such as simple shear extrusion [5], equal channel angular pressing [9], and accumulative roll bonding [11] are among the most attractive methods in this regard.

The basis of severe plastic deformation methods is applying pressure on a sample without changing its dimensions through various means. This ability to repeat the process for more cycles, achieve high strain values to introduce high-density dislocations, and ultimately lead to ultrafine-grained structures, is provided [9]. However, very few studies have resulted in the production of an industrial part using these methods, and most of these initiatives have remained at the level of research studies. This reality has diminished interest in conducting detailed investigations into alternative methods or seeking new methods that may be more efficient. In this article, a combination of two methods, powder metallurgy (PM) and simple shear extrusion (SSE), have been used for pure aluminum to eliminate defects created during the powder metallurgy process in the produced samples and align or enhance the properties of the final part compared to the cast sample.

2. Materials and Experimental Procedures

2.1. Materials

Aluminum powder with a purity of 99.5% and a particle size of 45 micrometers, along with the chemical composition and properties shown in Table 1, are used as the main material. H13 steel is used for the construction of the simple shear extrusion die, and CK45 steel is used for the powder metallurgy die in this study. The stages of the sample fabrication process are illustrated in Fig. 1.

2.2. Experiments

For the fabrication of test samples, 20 g of aluminum powder were used through the powder metallurgy method. High-quality molds and punches were employed to ensure complete surface quality during powder compression. After preparing the materials, the powder was poured into the mold and subjected to cold pressing using a press machine at a pressure of 45 megapascals. Following the powder compression and the production of the initial raw samples, these components were transferred to a tubular furnace model TF5/25-125050 under argon gas protection, and the sintering process was carried out. In the final step of this study, the produced samples with dimensions relevant to the channel of the simple shear extrusion die were cut using a wire cut EDM process at a speed of 1.0 mm. The passage channel of the samples in the die of the simple shear extrusion had a completely

Table 1. Specifications of the used aluminum powder

Material	Al	Si	Fe	Cu	Mn	V	Other	Density (g/cm^3)	Particle size (µm)
(%)	99.5	0.25	0.20	0.05	0.05	0.05	0.03	2.7	45

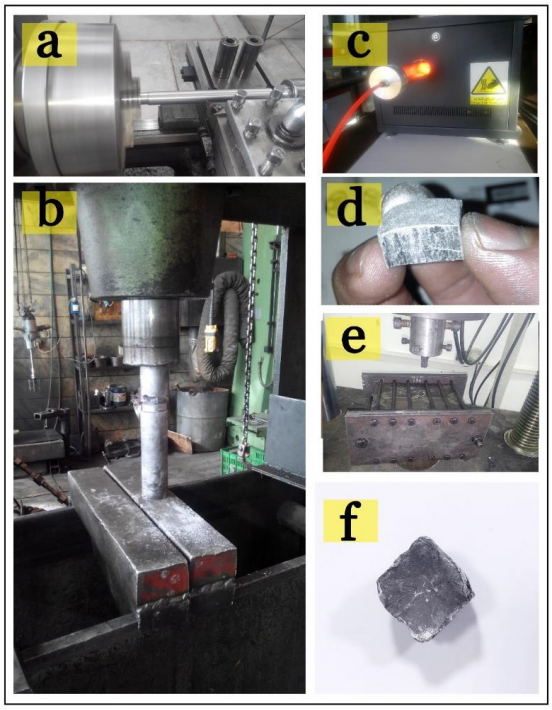

Fig. 1. Manufacturing process stages; (a) powder metallurgy mold manufacturing, (b) PM process, (c) tube furnace for sintering process, (d) powder metallurgy sample, (e) SSE die, and (f) extruded sample.

polished surface, and due to the importance of minimizing friction in severe plastic deformation processes, the samples were fully immersed in a soap solution as a lubricant before entering the channel. Finally, metallographic, hardness, wear, corrosion, and X-ray diffraction (XRD) were performed on the produced samples. XRD was conducted using an Explorer device manufactured by GNR Italy under the conditions V= 40 kV and current= 30 mA. To examine the phases present in the samples. In order to make morphological changes in the samples, field emission scanning electron microscopy (FESEM) using a MIRA3 model from TESCAN in the Czech Republic, with a resolution of up to 1.5 nanometers at 15 kilovolts was utilized. Sections perpendicular to the pressing direction that are designed for observing microstructure changes after sample fabrication, were examined using a reverse metallography microscope from Meiji, Japan. After surface finishing of the samples, a solution with a chemical composition containing 1% HNO_3, 65-75% H_3PO_4, and 5-10% CH_3COOH was used for surface etching. Subsequently, dry-pin-on-disk wear tests were conducted in a specialized laboratory according to ASTM G99 standard at room temperature under a force of 5 Newton, a time of 3600 seconds, and a speed of 60 revolutions per minute, using a steel pin as the indenter. The hardness of the samples was measured using the Brinell method with an INNOVATEST NEXUS 8000XL hardness tester, applying a 9.612 N tungsten carbide ball with a diameter of 2.5 mm and a holding time of 15 seconds according to ASTM A370 (2020) standard. The test was repeated three times for each sample to obtain an average value. Electrochemical corrosion tests were performed on the samples in the voltage range of -250 to +250 millivolts, a scan rate of 1 millivolt, and an OCP time of 1200 seconds.

3. Results and Discussion

3.1. Optical microscopy

The size and shape of grains are among the most critical factors affecting the properties and behavior of metals. It is well-known that the mechanical, chemical, biological, and superplastic behavior of metals at high temperatures, their corrosion behavior, and many of thier other properties, particularly their mechanical properties, depend on the grain size [12]. Metallographic results of the microstructure of samples produced by both methods are shown in Fig. 2. These images show that after simple extrusion cutting the sample has a more uniform and finer structure than the powder metallurgy-produced sample. Another structural difference between the two samples is the presence of gas pores in the powder metallurgy sample and the elimination of these pores in the extruded sample. One of the reasons for these results is related to the two-stage nature of the powder metallurgy method. In the powder metallurgy sample, due to the absence of force during sintering on the sample, gases resulting from moisture are easily released, leading to the formation of gas pores and a coarse-grained structure [13].

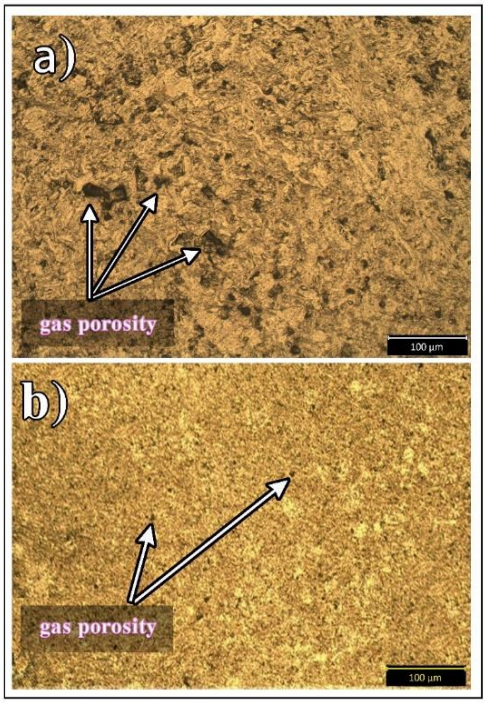

Fig. 2. Metallographic images; (a) powder metallurgy sample and (b) after one pass of SSE.

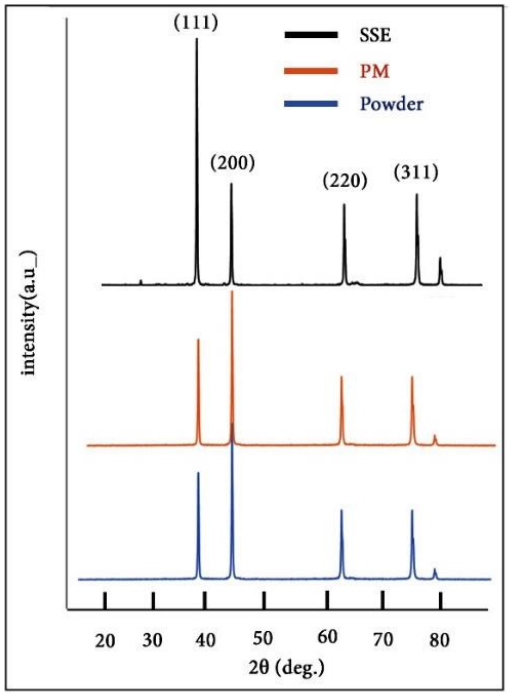

Fig. 3. XRD pattern of pure powder, powder metallurgy sample, and sample after simple shear extrusion.

3.2. XRD analysis

XRD analysis was performed on the samples to examine the phase changes and calculate the grain size and residual stresses during the two processes of powder metallurgy and simple extrusion cutting, as well as the initial powder. In Fig. 3, the XRD spectra is displayed. Based on the obtained results, it was found that the aluminum oxide (Al_2O_3) phase was not observed in the powder metallurgy-produced sample, which is attributed to the proper control of manufacturing conditions. As evident in Fig. 3, peaks at 38 and 40 degrees are identified as the strongest peaks present in aluminum. Additionally, weaker peaks at angles of 65 and 78 degrees are also observed. In XRD analysis, the broadening of the highest peak is mainly attributed to the small grain size and lattice distortion [14].

To visually illustrate the changes in the density of dislocations in the deformed sample, by approximating the peak profiles and strain broadening through Gaussian and Cauchy functions, the average grain size (d) can be determined from Eq. (1), and the microstrain (η) can be determined from Eq. (2) [15]:

$$\beta = \frac{k\,\lambda}{d\,cos\theta} \tag{1}$$

$$\frac{\beta^2}{tan^2\,\theta} = \frac{\lambda}{d}\left(\frac{\beta}{tan\,\theta\;sin\,\theta}\right) + 25\eta^2 \tag{2}$$

In which λ is the wavelength of X-ray radiation (λ= 0.154 nm), and θ and β are the angle and full width at half maximum (FWHM) of the largest peak, respectively. By performing a fitting for all measured peaks, after calculating d and η, the dislocation density (ρ) can be evaluated using Eq. (3) [14]:

$$\rho = \frac{2\sqrt{3}(\eta^2)^{1/2}}{b\times d} \tag{3}$$

In which b is the Burgers vector. Severe deformation of the specimen under the process of simple shear extrusion has a significant impact on the dislocation density that increases with the change in shape. Considering the results in Table 2 and for further discussion on the microsteucture in this work, SEM images of all three specimens are shown in Fig. 4. In these images, structural fractures are indicated with red arrows.

Table 2. Residual stress values obtained from XRD test

Parameter	PM	SSE
Burger vector (b)	2.871	2.871
Wavelength (λ)	0.154	0.154
Peak width – β (rad)	0.00174	0.00698
Peak angle – θ (rad)	0.41	0.40
Medium grain size – d (nm)	87.375	23.833
Thin strain – η (%)	0.0002	0.0011
Dislocation density – ρ (m^{-2})	0.0000015	0.0000754

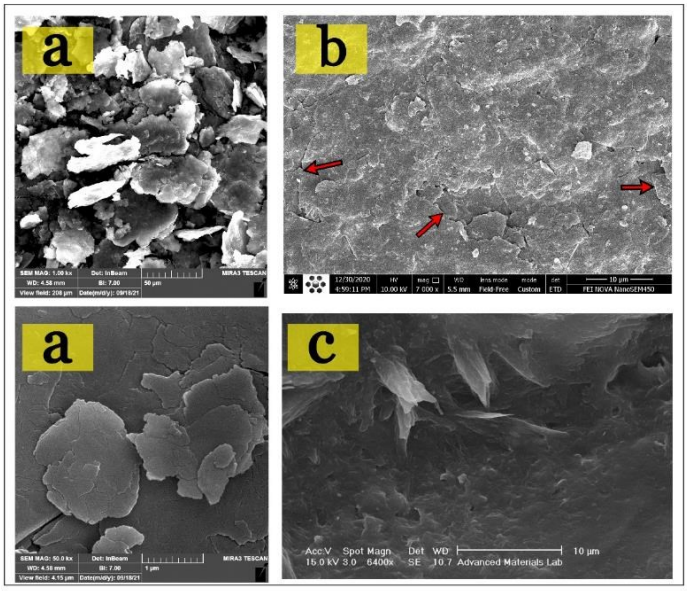

Fig. 4. SEM images of (a) initial powder, (b) powder metallurgy sample, and (c) sample after SSE.

3.3. Hardness test

In this study, the hardness of the as-cast raw specimen was 57 Brinell [17], which subsequently decreased to 29, 43, and 60.3 Brinell after the initial pressing, post-sintering, and simple shear extrusion, respectively. In contrast to the direction of powder metallurgy pressing, where Zabihi et al. [16], in a study on the production of pure aluminum specimens through the powder metallurgy method and subsequent severe plastic deformation using simple shear extrusion, were able to increase the hardness from 41 Brinell after sintering to a maximum of 46 Brinell after 3 passes of simple shear extrusion, in the present experiment, the pressing direction in both stages of powder metallurgy and simple shear extrusion was the same. The hardness-sensitivity results on the specimens at different stages are shown in Fig. 5.

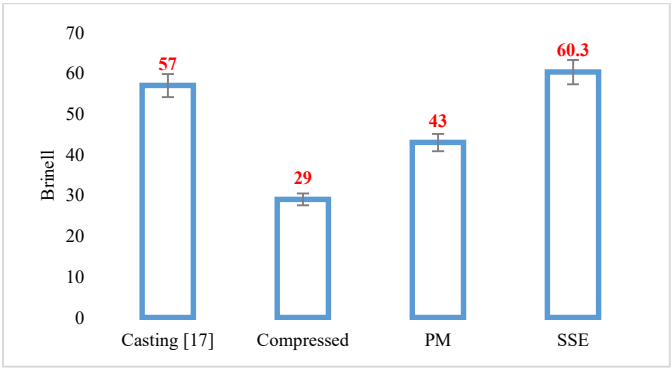

Fig. 5. Hardness test results in terms of brinell hardness.

This increase in hardness in the simple shear extrusion method is attributed to the homogeneous microstructure and smaller grain size of the specimen. Additionally, for a better understanding of hardness variations in aluminum, the hardness of cast aluminum is also reported [17].

3.4. Wear test

Figs. 6 and 7 show the weight loss after wear along with SEM images of the surfaces of the as-cast specimens and specimens produced by the powder metallurgy and simple shear extrusion methods under a 5 N load for 3600 seconds. The wear resistance in the simple shear extrusion specimen is lower than that in the powder metallurgy specimen, indicating an improvement in wear resistance. As observed, the results in the simple shear extrusion specimen display relatively smoother wear surfaces, and unlike the numerous deep grooves in the powder metallurgy specimen, in this case layer-by-layer and large-scale surface features are created. Therefore, the presence of grooved and layered areas along the wear path indicates that the dominant wear mechanisms in the simple shear extrusion specimen are: layering and abrasion. A comparison of the wear surfaces of the produced specimens showed a significant improvement in wear resistance for components produced by the simple shear extrusion method compared to the powder metallurgy specimen. This improvement can be attributed to the increased hardness and improved microstructure based on the production method. The reduction in grain size has led to an increase in wear resistance in the simple shear extrusion specimen. The results of weight loss after wear testing indicate that the maximum value for the simple shear extrusion specimen is 0.003 g, while this value reaches 0.02 g for the powder metallurgy specimen, which is a result of the softer and more abrasive nature of the powder metallurgy specimen.

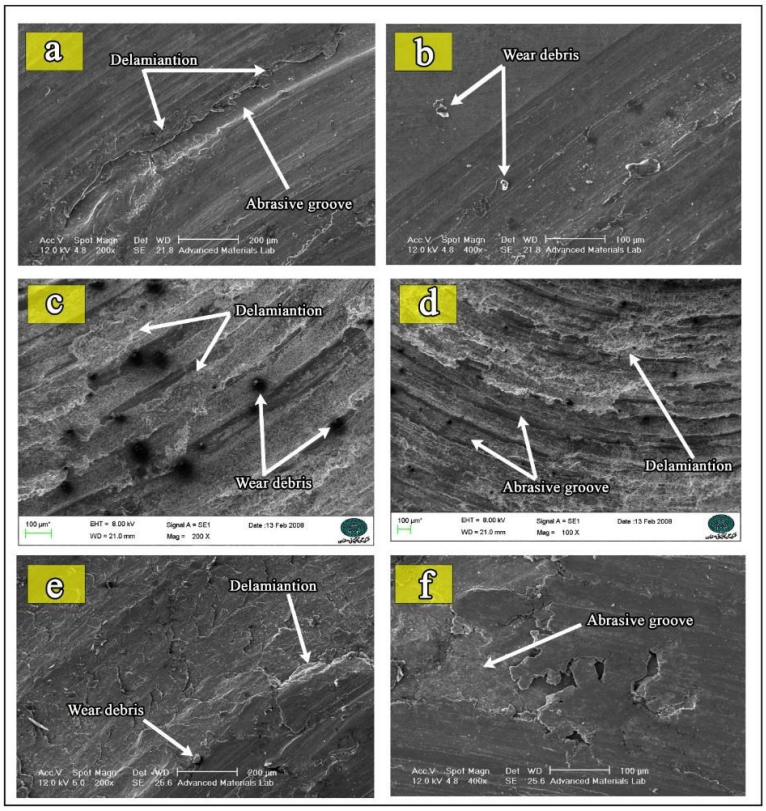

Fig. 6. SEM images; (a, b) cast sample, (c, d) powder metallurgy, and (e, f) after one pass of SSE.

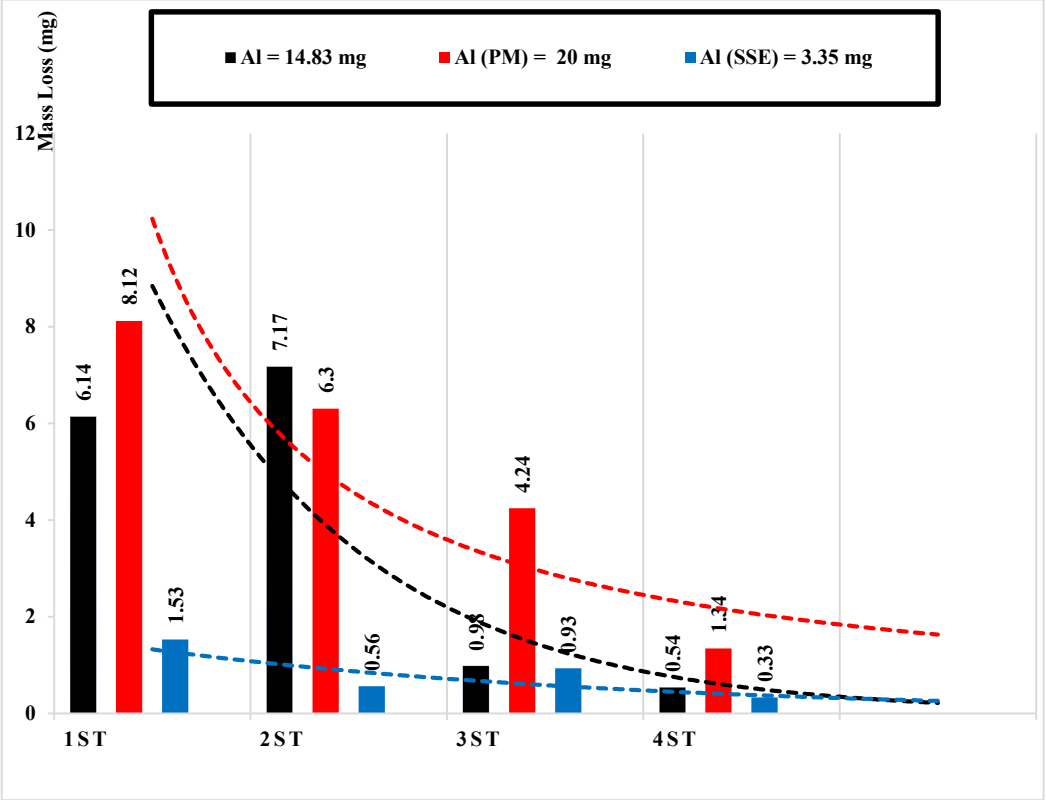

Fig. 7. Weight loss of produced samples after wear test.

3.5. Corrosion test

In Fig. 8, the potentiodynamic polarization corrosion test for the two specimens is presented. To measure corrosion, the Tafel slopes in the linear region of polarization curves are plotted, and the polarization resistance is calculated based on the Stern-Greay hypothesis and Eqs. (4-6) [18]:

$$R_p = \frac{b_a b_c}{2.303(b_a+b_c)i_{corr}} \quad (4)$$

$$i_{corr} = \frac{B}{R_p} \quad (5)$$

$$B = \frac{b_a b_c}{2.303(b_a+b_c)} \quad (6)$$

In the above equations, R_p is the polarization resistance (kohm.cm^2), b_a and b_c are the Tafel slopes for the anodic and cathodic branches, i_{corr} is the corrosion current density (μA/cm^2), and E_{corr} is the corrosion potential. The electrochemical parameters and corrosion rates are presented in Table 3. The values in this table indicate that the corrosion potential has increased from 730 mV in the powder metallurgy sample to 720 mV after simple extrusion, indicating a reduction in corrosion thermodynamically. Research has shown that if the corrosion potential increases and the current density has a descending trend, the corrosion process becomes self-inhibiting [19]. Therefore, as shown in Fig. 8, if the curve shifts to the right and downwards, the corrosion behavior improves. According to Table 3, the current density has decreased from 1.1 A/cm² for the powder metallurgy sample to 0.54 A/cm² in the simple shear extrusion sample. One of the best methods for comparing the corrosion resistance of materials is the LPR method. As shown in Table 3, the polarization resistance of the powder metallurgy sample is about 10.02 kohm.cm², while this value is approximately 1.18 kohm.cm² in the simple shear extrusion sample. This comparison indicates that the linear corrosion resistance of the simple shear extrusion sample is higher than that of the powder metallurgy sample. Furthermore, the corrosion rates of the extracted samples from the NOVA software are shown in Fig. 8 and Table 3. As clearly shown, the features of the simple extrusion method can reduce the corrosion rate.

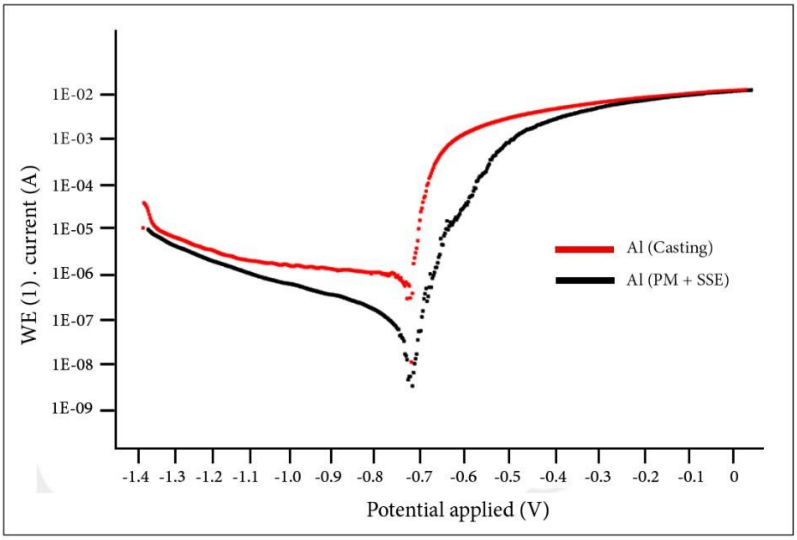

Fig. 8. Corrosion test results.

Table 3. Experimental results of the corrosion test

3.5% NaCl	Al (Casting)	SSE
β_a (V/dec)	0.0232	0.04188
β_c (V/dec)	0.18161	0.14301
i_{corr} (A/cm^2)	1.71 E^{-6}	1.54 E^{-6}
E_{corr} (V)	- 0.73	- 0.72
R_P (kohm/cm^2)	10.2	18.1
Corr. rate (mm/year)	0.018479	0.0016843

4. Conclusion

By taking into consideration the significance of metal matrix composites, this study focused on aluminum samples manufactured using a combination of powder metallurgy and simple shear extrusion, which are common and effective methods for producing metal matrix composites. The effects of these two processes on the microstructure and hardness of the produced samples were investigated, leading to the following conclusions:

1. According to the research results, severe plastic deformation methods enhance the mechanical properties and contribute to the relatively complete densification of composite samples produced by the powder metallurgy method.
2. Metallography results and SEM images of the produced samples indicate a reduction in grain size and a decrease in voids after using the simple extrusion method compared to the powder metallurgy method, resulting in increased hardness of the produced sample.
3. The recorded hardness values range from 57 Brinell for the raw cast sample to 29, 43, and 60.3 Brinell after initial pressing, sintering, and one pass of simple extrusion, respectively.
4. Wear test results also indicate a significant improvement in wear quality in the fine-grained sample. The weight loss after this test in the simple shear extrusion sample has decreased by 0.011 grams compared to the powder metallurgy stage.
5. Corrosion test results show a significant increase in the corrosion potential from 730 mV in the powder metallurgy sample to 720 mV after simple shear extrusion. The current density has decreased from 1.1 A/cm² for the powder metallurgy sample to 0.54 A/cm² in the SSE sample.

In conclusion, the combined powder metallurgy and SSE methods result in improved mechanical properties, densification, and wear resistance in aluminum-based metal matrix composites.

Acknowledgements

The authors are deeply grateful to all those who played a role in the success of this research.

Conflict of Interests

The authors declare that they have no known competing financial interests or personal relationships that could have appeared to influence this paper

Funding

The authors declare that no funds, grants, or other support were received during the preparation of this manuscript.

5. References

[1] Emmanuel, A. O., Fayomi, O. S. I., & Akande, I. G. (2021, April). Aluminium alloys as advanced materials: a short communication. In *IOP Conference Series: Materials Science and Engineering* (Vol. 1107, No. 1, p. 012024). IOP Publishing. https://doi.org/10.1088/1757-899X/1107/1/012024

[2] Liu, L., Zhao, G., Wang, G., Ma, X., Yan, Z., & Cao, S. (2023). Hot deformation behavior and microstructure evolution model of 7055 aluminum alloy. *Journal of Materials Research and Technology*, *27*, 3191-3213. https://doi.org/10.1016/j.jmrt.2023.10.165

[3] Lall, C., Heath, W. (2000). P/M aluminum structural parts: manufacturing and metallurgical fundamentals. *International Journal of Powder Metallurgy*, 36(6), 45-50.

[4] Abdullah, Y., & Kamarudin, N. (2012). Al/B4C composites with 5 and 10 wt% reinforcement content prepared by powder metallurgy. *Journal of Nuclear and Related Technologies*, *9*(01), 43-48.

[5] Sedehi, S. M. R., Khosravi, M., & Yaghoubinezhad, Y. (2021). Mechanical properties and microstructures of reduced graphene oxide reinforced titanium matrix composites produced by spark plasma sintering and simple shear extrusion. *Ceramics International*, *47*(23), 33180-33190. https://doi.org/10.1016/j.ceramint.2021.08.219

[6] Bunakov, N. A., Kozlov, D. V., Golovanov, V. N., Klimov, E. S., Grebchuk, E. E., Efimov, M. S., & Kostishko, B. B. (2016). Fabrication of multi-walled carbon nanotubes–aluminum matrix composite by powder metallurgy technique. *Results in Physics*, *6*, 231-232. https://doi.org/10.1016/j.rinp.2016.04.013

[7] Nassar, A. E., & Nassar, E. E. (2017). Properties of aluminum matrix nano composites prepared by powder metallurgy processing. *Journal of King Saud University-Engineering Sciences, 29*(3), 295-299. https://doi.org/10.1016/j.jksues.2015.11.001

[8] Dixit, M., & Srivastava, R. K. (2018, June). Effect of compaction pressure on microstructure, density and hardness of copper prepared by powder metallurgy route. In *IOP Conference Series: Materials Science and Engineering* (Vol. 377, No. 1, p. 012209). IOP Publishing. https://doi.org/0.1088/1757-899X/377/1/012209

[9] Rzepa, S., Trojanová, Z., Melzer, D., Procházka, R., Koukolíková, M., Podaný, P., & Džugan, J. (2023). Effect of ECAP on fracture toughness and fatigue endurance of DED-processed Ti-6Al-4V investigated on miniaturized specimens. *Journal of Alloys and Compounds*, *968*, 172167. https://doi.org/10.1016/j.jallcom.2023.172167

[10] Zhilyaev, A. P., & Langdon, T. G. (2008). Using high-pressure torsion for metal processing: Fundamentals and applications. *Progress in Materials Science, 53*(6), 893-979. https://doi.org/10.1016/j.pmatsci.2008.03.002

[11] Saito, Y., Tsuji, N., Utsunomiya, H., Sakai, T., & Hong, R. G. (1998). Ultra-fine grained bulk aluminum produced by accumulative roll-bonding (ARB) process. *Scripta Materialia, 39*(9), 1221-1227. https://doi.org/10.1016/S1359-6462(98)00302-9

[12] Langdon, T. G. (2007). The processing of ultrafine-grained materials through the application of severe plastic deformation. *Journal of Materials Science, 42*(10), 3388-3397. https://doi.org/10.1007/s10853-006-1475-8

[13] Sedehi, S. M. R., Khosravi, M., & Yaghoubi Nejad, Y. (2022). Experimental comparison of microstructure and surface properties of Al/Al2O3 sample produced by powder metallurgy and spark plasma sintering methods. *Journal of Solid and Fluid Mechanics, 12*(5), 123-132. https://doi.org/10.22044/JSFM.2022.11821.3580

[14] Liu, J., & Liang, C. (2017). Microstructure characterization and mechanical properties of bulk nanocrystalline aluminium prepared by SPS and followed by high-temperature extruded techniques. *Materials Letters*, *206*, 95-99. https://doi.org/10.1016/j.matlet.2017.06.129

[15] Zhou, F., Lee, J., Dallek, S., & Lavernia, E. J. (2001). High grain size stability of nanocrystalline Al prepared by mechanical attrition. *Journal of Materials Research, 16*(12), 3451-3458. https://doi.org/10.1557/JMR.2001.0474

[16] Zabihi, M., Emadoddin, E., & Qods, F. (2020). Processing of Al/Al_2O_3 composite using simple shear extrusion (SSE) manufactured by powder metallurgy (PM). *Metals and Materials International*, *26*, 1-13. https://doi.org/10.1007/s12540-019-00299-y

[17] Ribeiro, T. M., Catellan, E., Garcia, A., & dos Santos, C. A. (2020). The effects of Cr addition on microstructure, hardness and tensile properties of as-cast Al–3.8 wt.% Cu–(Cr) alloys. *Journal of Materials Research and Technology*, *9*(3), 6620-6631. https://doi.org/10.1016/j.jmrt.2020.04.054

[18] Cheng, L., Liu, C., Han, D., Ma, S., Guo, W., Cai, H., & Wang, X. (2019). Effect of graphene on corrosion

resistance of waterborne inorganic zinc-rich coatings. *Journal of Alloys and Compounds*, *774*, 255-264. https://doi.org/10.1016/j.jallcom.2018.09.315

[19] Zhang, Y., Chen, F., Zhang, Y., & Du, C. (2020). 1Influence of graphene oxide additive on the tribological and electrochemical corrosion properties of a PEO coating prepared on AZ31 magnesium alloy. *Tribology International*, *146*, 106135. https://doi.org/10.1016/j.triboint.2019.106135